Atmos. Chem. Phys., 9, 8189–8197, 2009
www.atmos-chem-phys.net/9/8189/2009/

Atmospheric Chemistry and Physics

Airborne measurements of the nitric acid partitioning in persistent contrails

D. Schäuble[1,2], C. Voigt[1,2], B. Kärcher[1], P. Stock[1], H. Schlager[1], M. Krämer[3], C. Schiller[3], R. Bauer[3], N. Spelten[3], M. de Reus[2], M. Szakáll[2], S. Borrmann[2,4], U. Weers[5], and Th. Peter[5]

[1]Deutsches Zentrum für Luft- und Raumfahrt, Institut für Physik der Atmosphäre, Oberpfaffenhofen, Germany
[2]Institut für Physik der Atmosphäre, Johannes-Gutenberg Universität Mainz, Mainz, Germany
[3]Institut für Stratosphärenforschung, FZ Jülich, Jülich, Germany
[4]Max-Planck-Institut für Chemie, Mainz, Germany
[5]Institut für Atmosphäre und Klima, ETH Zürich, Zürich, Switzerland

Received: 22 May 2009 – Published in Atmos. Chem. Phys. Discuss.: 30 June 2009
Revised: 6 October 2009 – Accepted: 12 October 2009 – Published: 2 November 2009

Abstract. This study reports the first systematic measurements of nitric acid (HNO_3) uptake in contrail ice particles at typical aircraft cruise altitudes. During the CIRRUS-III campaign cirrus clouds and almost 40 persistent contrails were probed with in situ instruments over Germany and Northern Europe in November 2006. Besides reactive nitrogen, water vapor, cloud ice water content, ice particle size distributions, and condensation nuclei were measured during 6 flights. Contrails with ages up to 12 h were detected at altitudes 10–11.5 km and temperatures 211–220 K. These contrails had a larger ice phase fraction of total nitric acid (HNO_3^{ice}/HNO_3^{tot} = 6%) than the ambient cirrus layers (3%). On average, the contrails contained twice as much HNO_3^{ice} as the cirrus clouds, 14 pmol/mol and 6 pmol/mol, respectively. Young contrails with ages below 1 h had a mean HNO_3^{ice} of 21 pmol/mol. The contrails had higher nitric acid to water molar ratios in ice and slightly higher ice water contents than the cirrus clouds under similar meteorological conditions. The differences in ice phase fractions and molar ratios between developing contrails and cirrus are likely caused by high plume concentrations of HNO_3 prior to contrail formation. The location of the measurements in the upper region of frontal cirrus layers might account for slight differences in the ice water content between contrails and adjacent cirrus clouds. The observed dependence of molar ratios as a function of the mean ice particle diameter suggests that ice-bound HNO_3 concentrations are controlled by uptake of exhaust HNO_3 in the freezing plume aerosols in young contrails and subsequent trapping of ambient HNO_3 in growing ice particles in older (age > 1 h) contrails.

Correspondence to: D. Schäuble
(dominik.schaeuble@dlr.de)

1 Introduction

Heterogeneous processes such as the uptake of nitric acid (HNO_3) in cirrus clouds influence the ozone budget in the tropopause region. Results from a global chemistry transport model indicate that HNO_3 uptake in cirrus ice particles and subsequent particle sedimentation has the potential to remove HNO_3 irreversibly from this region, leading to a large-scale reduction of gas phase HNO_3 concentrations (von Kuhlmann and Lawrence, 2006). Popp et al. (2004) and Krämer et al. (2008) suggest, based on in situ measurements, that tropical convective cirrus with a high ice water content have the highest potential to vertically redistribute HNO_3. Voigt et al. (2008) show that tropical cirrus clouds at low temperatures can also serve as nuclei for the formation of nitric acid trihydrate (NAT) particles. Kärcher (2005) demonstrates, based on cloud-resolving simulations, that long-lived Arctic frontal cirrus clouds are capable of denitrifying (and partially dehydrating) upper tropospheric air very efficiently at temperatures < 220 K over vertical regions as large as 3 km. Irreversible removal of gaseous HNO_3 reduces the concentrations of the ozone precursor nitrogen oxide (NO_x=NO+NO_2) and hence net ozone production rates at typical upper tropospheric NO_x levels. Meier and Hendricks (2002) address the sensitivity of this process by means of chemistry box model studies and find reductions in local ozone concentrations of up to 14%.

The interaction of HNO_3 and cirrus ice crystals was investigated experimentally during several field campaigns from the tropics to the Arctic (Weinheimer et al., 1998; Schlager et al., 1999; Kondo et al., 2003; Popp et al., 2004; Ziereis et al., 2004; Voigt et al., 2006). Voigt et al. (2006) summarized these measurements in terms of average nitric acid to water molar ratios ($\mu = HNO_3^{ice}/H_2O^{ice}$) in cirrus

ice particles and ice-bound fractions of total nitric acid ($\phi = HNO_3^{ice}/HNO_3^{tot}$). Kärcher and Voigt (2006) explained the inverse temperature trend of the μ and ϕ data by means of a model describing nitric acid uptake in growing ice crystals (trapping). Trapping refers to the combined effect of mass accomodation and desorption of molecules at an ice crystal surface that grows from the vapor phase by the deposition of water (H_2O) molecules, allowing for the burial of adsorbed molecules during surface layer growth. A recent update of the trapping model predicts the steady-state amount of HNO_3 trapped in bulk ice particles for a given ice growth rate, assuming Langmuir-type adsorption isotherms, including the underlying adsorption model asymptotically for non-growing ice particles (Kärcher et al., 2009).

Kärcher et al. (1996) simulate the formation of high levels of HNO_3 in jet aircraft exhaust plumes prior to contrail formation. These early HNO_3 concentrations are determined by the NO_x emission index and the engine exit plane concentration of the hydroxyl radical (OH) which acts as the primary oxidant. Arnold et al. (1992) and Tremmel et al. (1998) report the detection of gas phase HNO_3 in young aircraft exhaust plumes. Kärcher (1996) demonstrates by means of microphysical simulations that gaseous HNO_3 is efficiently transferred into plume aerosols and ice particles during contrail formation. Gao et al. (2004) measured HNO_3 in ice particles of a WB-57 aircraft contrail in the subtropics at 14–15 km altitude. They demonstrated that HNO_3 was present in contrail particles at temperatures below 205 K, presumably in the form of NAT, but did not explicitly report ice phase HNO_3 concentrations. An experimental quantification of the HNO_3 content in contrail ice particles as a function of mean ice particle size, a proxy for the microphysical age of persistent contrails, is lacking.

In this study, we present and interpret in situ observations of reactive nitrogen (NO_y), H_2O, as well as microphysical properties of contrails and thin frontal cirrus layers, performed over Germany, the North Sea, and the Baltic Sea during the CIRRUS-III campaign during 23–29 November 2006. During this campaign, the cirrus layers were probed with the Enviscope Learjet for almost 30 min in the temperature range 210–230 K (24, 28, and 29 November 2006) and 37 contrails were unintentionally sampled for more than 200 s at temperatures from 211 to 220 K (24 and 29 November). Contrail ages of up to about twelve hours were estimated based on the NO_y data (Schumann et al., 1998). These observations provide an unprecedented data set on the uptake of HNO_3 in persistent contrails.

2 Instrumentation

The Learjet performed 5 flights at latitudes between 48° N and 68° N with instruments measuring NO_y, H_2O, small ice crystal size distributions, and condensation nuclei (CN). The forward- and backward-facing inlets of the NO_y-instrument (Ziereis et al., 2000; Hegglin et al., 2006) operated by DLR and ETH Zurich sampled total (gas phase plus enhanced particulate) and gas phase NO_y, respectively. Total reactive nitrogen represents the sum of NO_x and other nitrogen-containing species in higher oxidation states, $NO_y = NO_x + HONO + HNO_3 + HO_2NO_2 + 2N_2O_5 + PAN + \ldots$. Two converter channels are located in the inlet system. Inside these gold tubes, heated to 300°C, NO_y is converted to NO using CO as the reducing agent (Fahey et al., 1985). The chemiluminescence of the reaction of NO with O_3 is detected with a photomultiplier at a rate of 1 Hz. Before each flight the conversion efficiency of the converters and the sensitivity of the chemiluminescence detector are determined by adding known amounts of NO_2 and NO, respectively. The instrument background is measured every ten minutes during the flight. Sampling of particulate NO_y with the forward-facing inlet depends on the ratio of the flow speed outside and inside the inlet tube as well as on the particle size. To calculate the concentration of particulate (in our case essentially ice phase) reactive nitrogen, $NO_y^{ice} = (NO_y^{forw} - NO_y^{back})/EF_{NO_y}$, we used the maximum enhancement factor $EF_{NO_y}^{max} = u_0/\overline{u} \approx 119 \pm 12$ (u_0 = aircraft true air speed, $\overline{u}$ = inlet flow speed; numerical values for 24 November) (Belyaev and Levin, 1974) for cirrus observations. This approximation may introduce errors of less than 8% in the EF_{NO_y} for observed ice crystal mean diameters ($d > 14\,\mu$m). In contrails containing smaller ice particles, we used a size-dependent relationship for $EF_{NO_y}(d)$ (Belyaev and Levin, 1974). Aerosol particles smaller than $1\,\mu$m in diameter were sampled with the forward- as well as the backward-facing inlet. Thus, they do not contribute to the NO_y^{ice} signal. Larger NO_y-containing aerosol particles, if present, are still likely smaller than most ice particles and are therefore associated with lower enhancement factors (~63% of $EF_{NO_y}^{max}$ for $d = 3\,\mu$m), resulting in a minor contribution to the NO_y^{ice} signal.

The NO_y detection limit in particles is 0.8 pmol/mol on 24 and 29 November and 0.6 pmol/mol on 28 November, as derived from the difference of the forward- and backward-facing channel signals outside clouds divided by the enhancement factor.

Nitric acid was not measured directly during CIRRUS-III, except during the flight on 28 November where we used a nylon filter in the aft-facing inlet to retain HNO_3 and thus derive the gas phase HNO_3/NO_y ratio. As the cirrus clouds on 24 and 29 November were detected slightly below the tropopause (ozone mixing ratios < 90 nmol/mol), we employed a value of 0.45 ± 0.2, corresponding to the mean gas phase HNO_3/NO_y ratio at these ozone levels during the flight on 28 November. Talbot et al. (1999) and Neuman et al. (2001) measured both HNO_3 and NO_y obtaining mean gas phase HNO_3/NO_y ratios of 0.35 and 0.2–0.5, respectively. However, they sampled at lower altitudes down to 8 and 7 km, respectively.

In young contrails NO_x constitutes the major fraction of NO_y. A microphysical plume model study (Meilinger et al., 2005) including detailed heterogeneous aerosol and ice phase chemistry indicates that the chemical conversion into HNO_3 is small in contrails in terms of the gas phase HNO_3/NO_y ratio ($\approx$1%) within the first ten hours after emission due to heterogeneous dehoxification and production of HONO. Entrainment of ambient HNO_3 is supposed to be the dominant process controlling the gas phase HNO_3 concentration in such contrails. Thus, we used the ambient HNO_3 concentration as an approximation for the concentration inside contrails. Further, we assumed that HNO_3 accounts for 100% of NO_y in ice particles in cirrus clouds as well as in contrails. N_2O_5 and HO_2NO_2 are quickly photolyzed during daytime and the uptake of PAN and HONO on ice crystals is probably small compared to HNO_3 (Bartels et al., 2002).

Total water (H_2O_{tot} = gas phase plus enhanced particulate water) was measured with the forward-facing inlet of the Fast In situ Stratospheric Hygrometer (FISH) (Zöger et al., 1999) using the Lyman-α photofragment fluorescence technique. Water vapor (H_2O) was detected with the OJSTER instrument (Open-path Jülich Stratospheric TDL ExpeRiment) (Schiller et al., 2008) by measuring the amount of laser light absorption in gaseous water molecules at a wavelength of 1.37 μm. The data of the OJSTER instrument were adjusted to the FISH instrument data in order to reach agreement in observations outside of clouds. On average, the OJSTER data were increased by 15 μmol/mol in cirrus clouds. The ice water content (IWC) was derived from IWC=(H_2O_{tot}-H_2O)/EF_{H_2O}. EF_{H_2O} was around 6 during CIRRUS-III. According to Schiller et al. (2008) the detection limit of the IWC is temperature dependent and averages to $\sim$0.1 mg m^{-3} in the range 210–230 K. The uncertainty in IWC is 15%.

The number concentration and size distribution of particles with diameters 2.8–29.2 μm were measured with the Forward Scattering Spectrometer Probe FSSP-100 (Borrmann et al., 2000). The particles were grouped into seven size bins and assumed to be spherical and composed of pure ice. The FSSP-100 data were used in combination with CN and NO_y measurements to identify contrails and cirrus (Sect. 3), i.e. to decide upon the presence or absence of ice crystals. Therefore, possible uncertainties associated with the FSSP-100 data are not critical for this purpose. We detected cirrus clouds from correlated increases in the FISH and FSSP-100 signals: cirrus clouds were observed either if the IWC was above 0.25 mg m^{-3} or if 0.1 mg m^{-3} < IWC < 0.25 mg m^{-3} and the FSSP-100 particle concentration > 0.

3 Identification of contrails

Contrails were identified from distinct simultaneous short-term increases in the time series of the concentrations of NO_y^{gas}, NO_y^{tot}, CN (> 5 nm diameter, not discussed here), and ice particles. The concurrence of these four signals and their strong increase and decrease within few seconds enabled a separation of contrails from cirrus clouds that were not recently affected by aviation. Lower limits of 0.1 nmol/mol for ΔNO_y^{gas} and 100 cm^{-3} for ΔCN were used as thresholds in this identification. These limits correspond to a contrail age of approximately 12 h assuming homogeneous dilution and sampling through the contrail core ($t[s] = (525[nmol/mol]/\Delta NO_y^{gas}[nmol/mol])^{1.25}$, Anderson et al., 1999). As contrails were not the primary focus of the CIRRUS-III campaign, we consider the spatial sampling to be random in terms of angles relative to the contrail axis and distances from the contrail core.

The amplitudes of the instrument peaks decrease with increasing contrail age and, for a given age, with distance from the contrail core. Contrails often exhibit significant spatial inhomogeneities in structure and dilution properties. The detection of contrails older than 12 h as well as the merging of several individual contrails may result in an extended contrail detection signal. Together, this introduces considerable uncertainty in the exact determination of contrail age from plume dilution data which is difficult to quantify.

We regard the probed cirrus clouds as upper tropospheric ice clouds that were not influenced by aircraft emissions within the last 12 h of their lifetime. It cannot be ruled out that part of the cirrus were actually older (age > 12 h) contrails. That being said, most of the observed contrails were embedded in thin cirrus clouds. In 79% of all cases either the FSSP or the FISH signal are > 0 before and after the contrail encounter which suggests the presence of ice crystals. 53% of the contrails were located in cirrus that meet the robust cirrus criterion mentioned in Sect. 2. This implies that for statistical reasons our data set does not allow us to compare properties of isolated contrails with those of contrails in cirrus clouds.

4 Nitric acid partitioning and ice water content in contrails

European Centre for Medium-Range Weather Forecasts analyses indicate that the upper regions of frontal cirrus layers were probed on 24 and 29 November, whereas on 28 November the observations originate from deeper inside cirrus clouds. On 24 November large parts of central Europe were covered by the cirrus. The cirrus layers were much more stretched out with a large North-South extension on 28 and 29 November. As an example of our suite of data, Fig. 1 shows a typical time series of data from the flight on 24 November over Germany. In this and the following section, we further present model results providing explanations of the observed uptake of HNO_3 in contrails and the cirrus layers.

Figure 2 (top panel) illustrates the decrease of the ice phase fraction of total nitric acid (ϕ) with increasing temperature.

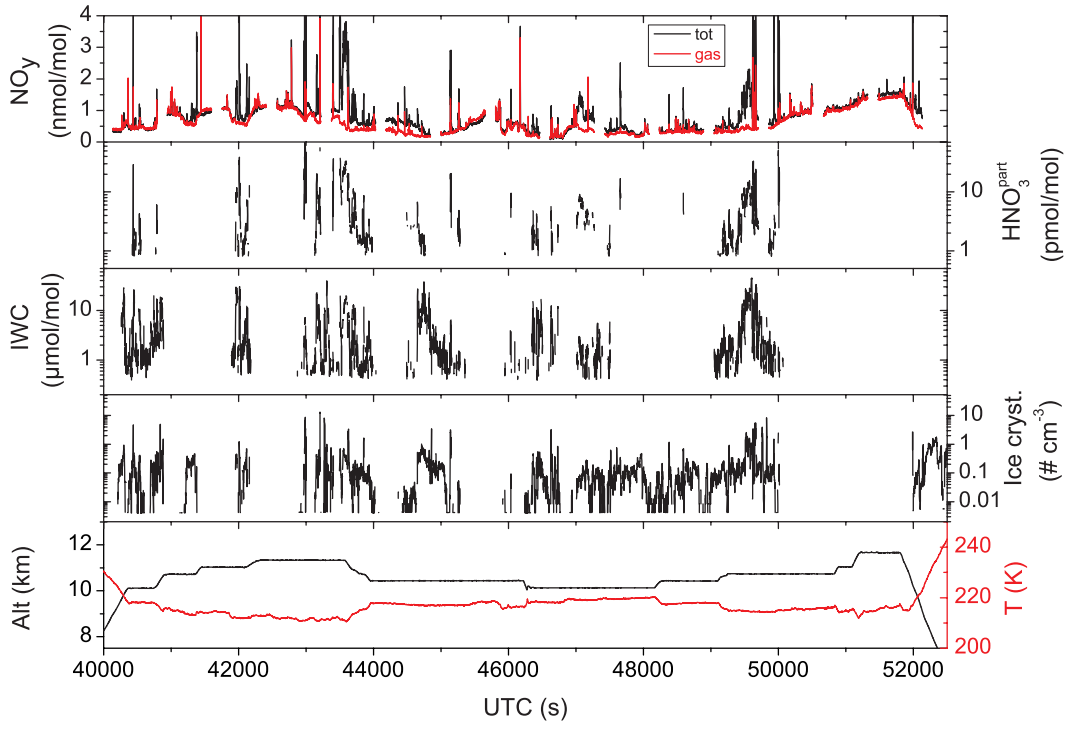

Fig. 1. Time series of gas phase and total NO_y (gas phase plus enhanced ice phase), ice phase HNO_3 volume mixing ratios, ice water content (IWC), number densities of ice particles with approximate diameters between 2.8 and 29.2 μm, as well as altitude and temperature for the flight on 24 November 2006. Gaps in the NO_y measurements are due to calibration procedures.

This dependence agrees with previous observations but almost all of the observed ϕ values in cirrus clouds (grey circles) are below the mean of previous measurements (Kärcher and Voigt, 2006). This is probably due to the relatively low IWCs measured during CIRRUS-III (Fig. 2, bottom panel) and the positive correlation between ϕ and IWC (Krämer et al., 2008). Further, the HNO_3 gas phase partial pressures were higher ($4.7\times10^{-8}\pm1.3\times10^{-8}$ hPa$\sim$0.2 nmol/mol) than the average of the other campaigns (2×10^{-8} hPa) (Kärcher and Voigt, 2006). The uncertainty of the gas phase HNO_3/NO_y ratio (Sect. 2) introduces an uncertainty in ϕ (time resolution 1 s) of about a factor of 2.

On average, contrails were found to have larger ϕ values than the cirrus layers under similar conditions (black and red squares, respectively). This is further illustrated with the help of probability distributions of ϕ displayed in Fig. 3a. At temperatures between 211 and 220 K, contrail ice particles contained on average 6% (cirrus 3%) of the total nitric acid. Twelve young contrails with $\Delta NO_y^{gas} > 0.75$ nmol/mol, corresponding to ages < 1 h, had even larger ice phase nitric acid fractions (9%). The maximum ϕ measured in contrails was 22%.

The gas phase equivalent mixing ratio of nitric acid in ice, HNO_3^{ice}, is 14 pmol/mol in contrails compared to 6 pmol/mol in the cirrus layers. The mean HNO_3^{ice} in the young contrails is 21 pmol/mol. Our finding that the absolute amount of HNO_3^{ice} in contrails is larger than in cirrus could be linked to differences in the ice formation process (Sect. 5).

Figure 2 (middle panel) shows the temperature dependence of the ice phase molar ratios of nitric acid and water (μ) in contrails (red circles) and in the surrounding cirrus layers (grey circles) that were not recently influenced by aviation. The μ values generally increase with decreasing temperature, as the probability of HNO_3 molecules to escape from the growing ice surfaces after adsorption is reduced at low temperatures leading to more efficient trapping of HNO_3 (Kärcher and Voigt, 2006).

The curves are results from a recent update of the trapping model now accounting for possible surface saturation upon adsorption at high ($> 2\times10^{-8}$ hPa) HNO_3 partial pressures (Kärcher et al., 2009), causing a weaker temperature dependence of μ than estimated by the previous model (Kärcher and Voigt, 2006). The dashed and solid model curves were computed for HNO_3 partial pressures of 3×10^{-8} hPa and 6×10^{-8} hPa, respectively, roughly capturing the range of measured values occurring in contrails and cirrus (see above). The trapping model bounds the observed mean μ values in cirrus (black squares) very well at 211–220 K. The model assumes temperature-dependent mean ice particle growth rates (net supersaturations) to estimate steady-state molar ratios. Deviations of individual data points from the mean model curves are likely caused by variable growth/sublimation histories of the observed ice

particles. Further, even in cirrus the μ of small ice crystals may be strongly influenced by the composition of the freezing aerosol (Sect. 5). As for the data points above 220 K, the low μ suggests that these ice particles have grown at low HNO_3 partial pressures. The relatively high IWC may imply that a considerable number of large ice crystals have sedimented from their formation region depleted in HNO_3 into the measurement region. Despite these non-local effects the data are still captured by the lower limit of trapping estimated in Kärcher and Voigt (2006).

The mean HNO_3/H_2O molar ratio in contrails of 4×10^{-6} is found to be approximately twice as large as in the cirrus layers (2×10^{-6}), which is illustrated by means of the probability distribution of μ (Fig. 3b) . The increase in mean μ is mainly caused by the data points below 215 K, compare red and black squares in Fig. 2 (middle panel). This difference is roughly consistent with the difference in the mean HNO_3^{ice} per particle (see above).

The IWC of contrails and cirrus clouds versus temperature is shown in Fig. 2 (bottom panel). Compared to the comprehensive compilation of IWCs by Schiller et al. (2008), based on a large number of in situ measurements at midlatitudes (mean values indicated by the solid curve), the IWC observations on 24 and 29 November below 220 K appear to be slightly lower for the following reasons. First, thin ice clouds with IWCs as low as 0.1 mg m^{-3} were included in our data set derived from simultaneous FSSP and total water increases. In addition, in the upper region of frontal cirrus layers, where the data were taken, ice nucleation is supposed to take place and sedimentation of large ice particles out of these layers keeps the IWC small. Finally, there may be entrainment of dry air from above and a reduced IWC arises while crossing cloud free patches within the 200 m (1 s) measurement interval. The solid curve marks the average values obtained by probing the whole vertical extension of a population of cirrus clouds (Schiller et al., 2008) and is therefore located above our mean IWCs (black squares) below 220 K. Above 220 K our IWC data were taken deeper inside a cirrus cloud and the respective means are therefore in better agreement with the solid curve. The fact that the trapping model seems to overpredict μ at higher temperatures (curves not shown in Fig. 2, middle panel) may be tied to the impact of sedimentation and more strongly varying ambient conditions throughout the probed cirrus clouds, which is much less pronounced in the upper layers probed at lower temperatures.

The contrails have a slightly larger mean IWC (red squares) than the cirrus clouds, 1.8 and 1.3 mg m^{-3}, respectively. The IWC of young contrails 2.9 mg m^{-3} is more than twice the cirrus mean. According to plume dilution estimates derived from large-eddy simulations of aircraft wake vortex development (Gerz et al., 1998), the H_2O aircraft emissions become unimportant for contrails older than a few minutes. So most of the H_2O in contrail ice condenses from the ambient air during ice particle growth and differences between contrail and cirrus IWCs are expected to diminish over time.

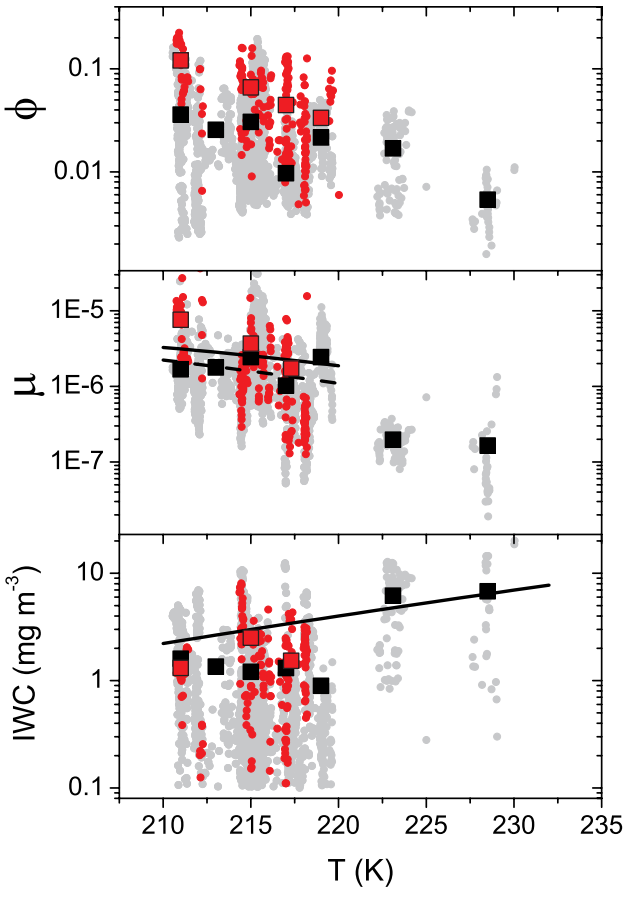

Fig. 2. The temperature dependence of the (top) ice phase fraction of total nitric acid ($\phi = HNO_3^{ice}/HNO_3^{tot}$), (middle) molar ratio of nitric acid to water in ice particles ($\mu = HNO_3^{ice}/H_2O^{ice}$), and (bottom) ice water content (IWC) of contrails (red circles) and cirrus clouds (grey circles). Squares are means over 2 K temperature bins. For μ and IWC in contrails the warmest bin is centered at 217.3 K (instead of 217 K) to comprise the measurements at temperatures slightly higher than 218 K. Curves in the middle panel are results from the trapping model evaluated at HNO_3 partial pressures of 3×10^{-8} hPa (dashed curve) and 6×10^{-8} hPa (solid curve) at temperatures where contrails were detected (Kärcher et al., 2009). The curve in the bottom panel depicts the mean cirrus IWCs based on a large number of in situ measurements at midlatitudes (Schiller et al., 2008).

We additionally report a striking difference between measured contrail and cirrus cloud ice particle number densities in the FSSP-100 size range 2.8–29.2 μm in diameter, 1.5 cm^{-3} and 0.2 cm^{-3}, respectively. We are aware of the fact that shattering of large ($d > 50\,\mu$m) ice crystals at the front end of the FSSP instrument may artificially enhance the measured number concentrations (Heymsfield, 2007; De Reus et al., 2009). However, shattering is probably not affecting the above values to a great extent, as the concentrations of such large particles in the contrails and

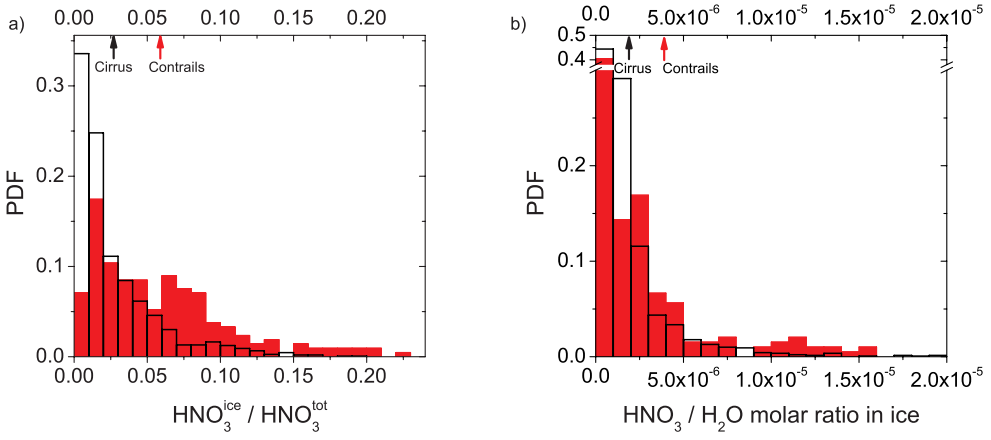

Fig. 3. Normalized probability density functions of the ice phase fraction of total HNO_3 ϕ **(a)** and the HNO_3/H_2O molar ratio in ice μ **(b)** for contrails (red) and cirrus clouds (transparent). Arrows indicate the means for the temperature range (211–220 K) where contrails occurred.

in the nucleation layers of cirrus are presumably very small (Schröder et al., 2000). More robust conclusions would be possible when using cloud probes unaffected by shattering and extending the size distribution measurements to diameters $> 30\,\mu$m.

5 Nitric acid uptake in developing contrails

Given the limited amount of contrail data, it is unclear whether the systematic differences in ice phase fraction and molar ratios in ice presented in Sect. 4 are representative. Nevertheless, sorting the molar ratio data as a function of the mean ice particle size enables us to study the HNO_3 uptake process in contrails in more detail.

Figure 4 shows the molar ratios (grey circles) along with the mean (black squares) and median (grey squares) values of the contrails probed during CIRRUS-III as a function of the mean ice particle diameter. We associate rough estimates of the contrail age with the mean diameter, as indicated in the figure. The contrail age is calculated according to Sect. 3 and linked to the mean ice crystal diameter with a linear regression for contrails younger than 1 h. In persistent contrails, the mean size increases due primarily to uptake of H_2O from the gas phase (depositional growth). The measurements show a clear trend of decreasing μ with increasing mean size or age. Young contrails with ages 10–15 min and mean diameters $\sim 7\,\mu$m have a mean $\mu \approx 10^{-5}$, while older contrails with ages > 1 h and mean diameters > 10–$15\,\mu$m exhibit values closer to the mean $\sim 2\times10^{-6}$ of the cirrus data.

Using campaign-average contrail temperature (216 K) and HNO_3 partial pressure ($\sim 5\times10^{-8}$ hPa), the updated trapping model (Kärcher et al., 2009) predicts an average molar ratio $\mu_\infty \approx 2\times10^{-6}$ (dash-dotted curve), consistent with the cirrus observations (middle panel in Fig. 2 and Fig. 3b) and the older contrail data in Fig. 4. Increasing the partial pressure would not significantly increase μ because the adsorption of HNO_3 becomes limited by a monolayer surface coverage during trapping. Hence, trapping of low levels of entrained ambient HNO_3 by the growing contrail ice particles is not capable of explaining the high molar ratios exceeding 10^{-5} in young contrails.

How are the high molar ratios brought about? We argue that a high concentration of HNO_3 had already entered the ice particles during contrail formation, when they are very small (mean diameters $\sim 1\,\mu$m), leading to very high molar ratios. Subsequent depositional growth increases the size per ice particle, while trapping in young contrails (mean diameters 1–10 μm) only adds a small contribution to the HNO_3 content per particle; both effects cause μ to decrease in this phase of contrail development. Further growth to larger sizes diminishes the role of the initially high molar ratios and trapping takes over the dominant part in determining μ. These processes are illustrated by the model curves as explained below.

Before we quantify the modeled μ dependence shown in Fig. 4 in more detail, we note that similar arguments were used to explain the in situ observations of high molar ratios of $\sim 5\times10^{-5}$ in nascent cirrus ice particles forming and growing at temperatures near 202 K and HNO_3 partial pressures similar to those encountered during CIRRUS-III (Voigt et al., 2007). In this case, it was proposed that sulfate aerosol particles dissolve large amounts of gaseous HNO_3 prior to freezing. Assuming that about half of the dissolved HNO_3 remained in the ice particles after freezing, this led to initial molar ratios ~ 0.01. We suggest that the same processes act in contrails.

Freezing aerosol surface areas, ice supersaturations, and HNO_3 partial pressures are higher during contrail formation than during cirrus formation. Contrail ice particles form from plume particles that efficiently dissolve exhaust HNO_3 prior to ice formation (Kärcher, 1996). We estimate the nitric acid to water molar ratio to be $\mu_0 \approx 0.03$ in the freezing plume

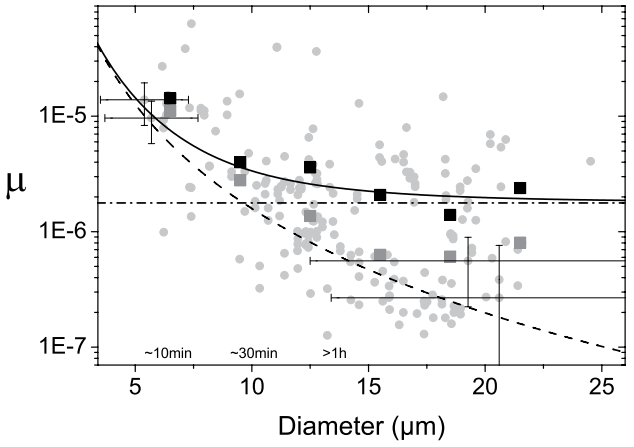

Fig. 4. Molar ratios of nitric acid to water in contrail ice particles μ versus mean ice particle diameter. Black (grey) squares represent means (medians) over 3 μm size bins. For illustration, four data points are displayed with estimated measurement errors. Diameters $> 20\,\mu$m are uncertain due to the large-size cut-off of the FSSP-100. Approximate contrail ages are inferred from the gas phase ΔNO_y data. Curves are model results; solid curve according to Eq. (1), dash and dash-dotted curves indicate limiting cases; see text for details.

aerosol particles as in Voigt et al. (2007), assuming an equilibrium composition of aqueous sulfuric acid droplets (diameter $d_0 = 0.75\,\mu$m) at 215 K and an HNO_3 partial pressure 2×10^{-6} hPa (corresponding to 10 nmol/mol) consistent with plume chemistry simulations (Kärcher et al., 1996). This value roughly determines the initial molar ratio of the nascent contrail ice particles. The resulting evolution of μ in the contrail as a function of the mean ice particle diameter d (solid curve in Fig. 4) is given by (Kärcher and Voigt, 2006; Voigt et al., 2007):

$$\mu = \mu_0 \frac{1}{1+N} + \mu_\infty \frac{N}{1+N}, \quad N = \kappa \left(\frac{d}{d_0}\right)^3, \tag{1}$$

with the ratio of ice and freezing aerosol particle bulk mass densities κ, the initial ice particle diameter d_0, and the trapped molar ratio μ_∞ as derived above. The ice particle dilution factor N quickly takes values $\gg 1$ due to depositional growth. The first part of this relationship describes the initial decrease of $\mu \propto 1/d^3$ by uptake of H_2O (dashed curve); it becomes smaller than the second (trapping) contribution for $d > 10\,\mu$m, at which point the trapped amount (dash-dotted curve) is approached, $\mu \to \mu_\infty$.

Except during the very short initial growth phase after ice nucleation, cirrus particles are usually large enough to render the aerosol component in Eq. (1) unimportant relative to the trapping component (Kärcher and Voigt, 2006). As shown here, the aerosol component is more prominent in persistent contrails, because mean contrail ice particle diameters stay relatively small owing to the large number density of ice particles compared to cirrus. Given the measurement uncertainties, the simple uptake model explains the observed trend in the mean values $\mu(d)$ in developing contrails fairly well. Variability in initial and ambient conditions may explain deviations of individual data points from the mean model curve. A set of data points between 10–20 μm following the median values seems to be well fitted by the dashed curve without trapping. We speculate that those measurements might be more representative of supersaturated inner contrail regions in which the local HNO_3 gas phase mixing ratio was small due to inefficient mixing from ambient air.

6 Summary and conclusions

During the CIRRUS-III field campaign gas phase and ice phase reactive nitrogen, ice water content, and ice crystal size distributions were measured in contrails and cirrus at midlatitudes close to the tropopause. The temperatures and HNO_3 partial pressures were in the ranges 210–230 K and $3–6\times10^{-8}$ hPa, respectively. The observed uptake of HNO_3 in ice particles residing in the upper layers of frontal cirrus clouds confirms previous results from airborne field campaigns carried out in polar, midlatitude, and sub-tropical regions (Voigt et al., 2006).

On average the probed contrails contained twice as much ice-bound HNO_3 as the cirrus clouds within 211–220 K, 14 pmol/mol and 6 pmol/mol, respectively. Thus, the mean fraction of total HNO_3 in ice particles was considerably larger in the contrails (6%) than in the cirrus layers (3%). In young contrails (approximate age < 1 h) this fraction was even higher (9%). The measured molar ratios of HNO_3 and H_2O in contrail ice particles exceeded 10^{-5} for small particle sizes, or contrail ages. For older contrails, molar ratios approached the mean value of 2×10^{-6} detected in the cirrus layers. Averaged over all detected contrails regardless of age, this caused the mean molar ratios in contrails to be about twice as large as in the cirrus clouds.

Motivated by our study, contrails may be regarded as an atmospheric laboratory to study HNO_3 uptake during ice particle growth. Our data show that ice phase HNO_3/H_2O molar ratios decrease during contrail ageing. This dependence was explained by uptake of high levels of HNO_3 into the freezing aerosol particles during ice formation in contrails and subsequent trapping of relatively low levels of ambient HNO_3 in growing contrail ice particles. In young contrails with ages < 1 h or mean diameters $< 10\,\mu$m, the ice phase HNO_3 concentrations are therefore largely controlled by the jet engine NO_x and OH emission indices. More airborne measurements with extended instrumentation are needed to study the dependence of HNO_3 uptake on HNO_3 partial pressure and to better quantify ice particle size distributions in developing contrails.

The results of this study help constrain chemical-microphysical models simulating heterogeneous chemistry in persistent contrails in order to constrain the impact of

plume processing of NO_x emissions on the chemical production or loss of ozone. Chemistry transport model simulations suggest that net upper tropospheric ozone production rates may decrease by ∼15–18% in the main midlatitude Northern Hemisphere traffic areas due to decreased aircraft-induced NO_x perturbations when chemical plume processing effects are accounted for (Kraabøl et al., 2002). Uptake of HNO_3 in contrail ice particles may further reduce ozone production by passivating NO_x.

Acknowledgements. This work was carried out within the HGF-junior research group AEROTROP (Impact of Aircraft Emissions on the heteROgeneous chemistry of the TROPopause region) and the DLR-project CATS (Climate-compatible Air Transport System). Part of this work was funded by the EU integrated project SCOUT O3 and the DFG SPP HALO 1294. The CIRRUS-III campaign was organized and mainly financed by FZ Jülich and the German Science Foundation (SFB 641 – The Tropospheric Ice Phase) and supported by DLR, the Max Planck Society, ETH Zurich, and Droplet Measurement Technology Inc. (Boulder, CO, USA). We thank Enviscope GmbH and the pilots and technicians of the Gesellschaft für Flugzieldarstellung (Hohn, Germany) for technical and logistical support during the campaign. We are grateful to M. Krämer for the organization of the campaign and to P. Spichtinger, F. Weidle, and G. Günther for the successful flight planning. We acknowledge fruitful discussions with D. Fahey.

Edited by: V. F. McNeill

References

Anderson, B. E., Cofer, W. R., Crawford, J., Gregory, G. L., Vay, S. A., Brunke, K. E., Kondo, Y., Koike, M., Schlager, H., Baughcum, S. L., Jensen, E., Zhao, Y., and Kita, K.: An assessment of aircraft as a source of particles to the upper troposphere, Geophys. Res. Lett., 26, 3069–3072, 1999.

Arnold, F., Scheid, J., Stilp, T., Schlager, H., and Reinhardt, M. E.: Measurements of jet aircraft emissions at cruise altitude I: the odd- nitrogen gases NO, NO_2, HNO_2 and HNO_3, Geophys. Res. Lett., 19, 2421–2424, 1992.

Bartels, T., Eichler, B., Zimmermann, P., Gäggeler, H. W., and Ammann, M.: The adsorption of nitrogen oxides on crystalline ice, Atmos. Chem. Phys., 2, 235–247, 2002, http://www.atmos-chem-phys.net/2/235/2002/.

Belyaev, S. P. and Levin, L. M.: Techniques for collection of representative aerosol samples, J. Aerosol Sci., 5, 325–338, 1974.

Borrmann, S., Luo, B., and Mishchenko, M.: Application of the T-matrix method to the measurement of aspherical (ellipsoidal) particles with forward scattering optical particle counters, J. Aerosol Sci., 31, 789–799, 2000.

de Reus, M., Borrmann, S., Bansemer, A., Heymsfield, A. J., Weigel, R., Schiller, C., Mitev, V., Frey, W., Kunkel, D., Kürten, A., Curtius, J., Sitnikov, N. M., Ulanovsky, A., and Ravegnani, F.: Evidence for ice particles in the tropical stratosphere from in-situ measurements, Atmos. Chem. Phys., 9, 6775–6792, 2009, http://www.atmos-chem-phys.net/9/6775/2009/.

Fahey, D. W., Eubank, C. S., Hubler, G., and Fehsenfeld, F. C.: Evaluation of a catalytic reduction technique for the measurement of total reactive odd-nitrogen NO_y in the atmosphere, J. Atmos. Chem., 3, 435–468, 1985.

Gao, R. S., Popp, P. J., Fahey, D. W., Marcy, T. P., Herman, R. L., Weinstock, E. M., Baumgardner, D., Garrett, T. J., Rosenlof, K. H., Thompson, T. L., Bui, T. P., Ridley, B. A., Wofsy, S. C., Toon, O. B., Tolbert, M. A., Kärcher, B., Peter, T., Hudson, P. K., Weinheimer, A. J., and Heymsfield, A. J.: Evidence that nitric acid increases relative humidity in low-temperature cirrus clouds, Science, 303, 516–520, 2004.

Gerz, T., Dürbeck, T., and Konopka, P.: Transport and effective diffusion of aircraft emissions, J. Geophys. Res., 103, 25905–25913, 1998.

Hegglin, M. I., Brunner, D., Peter, T., Hoor, P., Fischer, H., Staehelin, J., Krebsbach, M., Schiller, C., Parchatka, U., and Weers, U.: Measurements of NO, NO_y, N_2O, and O_3 during SPURT: implications for transport and chemistry in the lowermost stratosphere, Atmos. Chem. Phys., 6, 1331–1350, 2006, http://www.atmos-chem-phys.net/6/1331/2006/.

Heymsfield, A. J.: On measurements of small ice particles in clouds, Geophys. Res. Lett., 34, L23812, doi:10.1029/2007GL030951, 2007.

Kärcher, B.: Aircraft-generated aerosols and visible contrails, Geophys. Res. Lett., 23, 1933–1936, 1996.

Kärcher, B.: Supersaturation, dehydration, and denitrification in Arctic cirrus, Atmos. Chem. Phys., 5, 1757–1772, 2005, http://www.atmos-chem-phys.net/5/1757/2005/.

Kärcher, B., Abbatt, J. P. D., Cox, R. A., Popp, P. J., and Voigt, C.: Trapping of trace gases by growing ice surfaces including surface-saturated adsorption, J. Geophys. Res., 114, D13306, doi:10.1029/2009JD011857, 2009.

Kärcher, B., Hirschberg, M. M., and Fabian, P.: Small-scale chemical evolution of aircraft exhaust species at cruising altitudes, J. Geophys. Res., 101, 15169–15190, 1996.

Kärcher, B. and Voigt, C.: Formation of nitric acid/water ice particles in cirrus clouds, Geophys. Res. Lett., 33, L08806, doi:10.1029/2006GL025927, 2006.

Kondo, Y., Toon, O. B., Irie, H., Gamblin, B., Koike, M., Takegawa, N., Tolbert, M. A., Hudson, P. K., Viggiano, A. A., Avallone, L. M., Hallar, A. G., Anderson, B. E., Sachse, G. W., Vay, S. A., Hunton, D. E., Ballenthin, J. O., and Miller, T. M.: Uptake of reactive nitrogen on cirrus cloud particles in the upper troposphere and lowermost stratosphere, Geophys. Res. Lett., 30, 1154, doi:10.1029/2002GL016539, 2003.

Kraabøl, A. G., Berntsen, T. K., Sundet, J. K., and Stordal, F.: Impacts of NO_x emissions from subsonic aircraft in a global three-dimensional chemistry transport model including plume processes, J. Geophys. Res., 107, 4655, doi:10.1029/2001JD001019, 2002.

Krämer, M., Schiller, C., Voigt, C., Schlager, H., and Popp, P. J.: A climatological view of HNO_3 partitioning in cirrus clouds, Q. J. Roy. Meteorol. Soc., 134, 905–912, 2008.

Meier, A. and Hendricks, J.: Model studies on the sensitivity of upper tropospheric chemistry to heterogeneous uptake of HNO_3 on cirrus ice particles, J. Geophys. Res., 107, 4696, doi:10.1029/2001JD000735, 2002.

Meilinger, S. K., Kärcher, B., and Peter, Th.: Microphysics and heterogeneous chemistry in aircraft plumes – high sensitivity on local meteorology and atmospheric composition, Atmos. Chem. Phys., 5, 533–545, 2005,

http://www.atmos-chem-phys.net/5/533/2005/.

Neuman, J. A., Gao, R. S., Fahey, D. W., Holecek, J. C., Ridley, B. A., Walega, J. G., Grahek, F. E., Richard, E. C., McElroy, C. T., Thompson, T. L., Elkins, J. W., Moore, F. L., and Ray, E. A.: In situ measurements of HNO_3, NO_y, NO, and O_3 in the lower stratosphere and upper troposphere, Atmos. Environ., 35, 5789–5797, 2001.

Popp, P. J., Gao, R. S., Marcy, T. P., Fahey, D. W., Hudson, P. K., Thompson, T. L., Kärcher, B., Ridley, B. A., Weinheimer, A. J., Knapp, D. J., Montzka, D. D., Baumgardner, D., Garrett, T. J., Weinstock, E. M., Smith, J. B., Sayres, D. S., Pittman, J. V., Dhaniyala, S., Bui, T. P., and Mahoney, M. J.: Nitric acid uptake on subtropical cirrus cloud particles, J. Geophys. Res., 109, D06302, doi:10.1029/2003JD004255, 2004.

Schiller, C., Krämer, M., Afchine, A., Spelten, N., and Sitnikov, N.: Ice water content of Arctic, midlatitude, and tropical cirrus, J. Geophys. Res., 113, D24208, doi:10.1029/2008JD010342, 2008.

Schlager, H., Petzold, A., Ziereis, H., Dörnbrack, A., Grimm, F., Arnold, F., and Schiller, C.: In-situ observations of particulate NO_y in cirrus clouds for different atmospheric conditions, in: Proceedings of the European Workshop on Aviation, Aerosols, Contrails, and Cirrus Clouds, edited by: Schumann, U. and Amanatidis, G. T., European Commission, Brussels, Seeheim, Germany, 68–73, 1999.

Schröder, F., Kärcher, B., Duroure, C., Ström, J., Petzold, A., Gayet, J. F., Strauss, B., Wendling, P., and Borrmann, S.: On the transition of contrails into cirrus clouds, J. Atmos. Sci., 57, 464–480, 2000.

Schumann, U., Schlager, H., Arnold, F., Baumann, R., Haschberger, P., and Klemm, O.: Dilution of aircraft exhaust plumes at cruise altitudes, Atmos. Environ., 32, 3097–3103, 1998.

Talbot, R. W., Dibb, J. E., Scheuer, E. M., Kondo, Y., Koike, M., Singh, H. B., Salas, L. B., Fukui, Y., Ballenthin, J. O., Meads, R. F., Miller, T. M., Hunton, D. E., Viggiano, A. A., Blake, D. R., Blake, N. J., Atlas, E., Flocke, F., Jacob, D. J., and Jaegle, L.: Reactive nitrogen budget during the NASA SONEX mission, Geophys. Res. Lett., 26, 3057–3060, 1999.

Tremmel, H. G., Schlager, H., Konopka, P., Schulte, P., Arnold, F., Klemm, M., and Droste-Franke, B.: Observations and model calculations of jet aircraft exhaust products at cruise altitude and inferred initial OH emissions, J. Geophys. Res., 103, 10803–10816, 1998.

Voigt, C., Kärcher, B., Schlager, H., Schiller, C., Krämer, M., de Reus, M., Vössing, H., Borrmann, S., and Mitev, V.: In-situ observations and modeling of small nitric acid-containing ice crystals, Atmos. Chem. Phys., 7, 3373–3383, 2007, http://www.atmos-chem-phys.net/7/3373/2007/.

Voigt, C., Schlager, H., Roiger, A., Stenke, A., de Reus, M., Borrmann, S., Jensen, E., Schiller, C., Konopka, P., and Sitnikov, N.: Detection of reactive nitrogen containing particles in the tropopause region – evidence for a tropical nitric acid trihydrate (NAT) belt, Atmos. Chem. Phys., 8, 7421–7430, 2008, http://www.atmos-chem-phys.net/8/7421/2008/.

Voigt, C., Schlager, H., Ziereis, H., Kärcher, B., Luo, B. P., Schiller, C., Krämer, M., Popp, P. J., Irie, H., and Kondo, Y.: Nitric acid in cirrus clouds, Geophys. Res. Lett., 33, L05803, doi:10.1029/2005GL025159, 2006.

von Kuhlmann, R. and Lawrence, M. G.: The impact of ice uptake of nitric acid on atmospheric chemistry, Atmos. Chem. Phys., 6, 225–235, 2006, http://www.atmos-chem-phys.net/6/225/2006/.

Weinheimer, A. J., Campos, T. L., Walega, J. G., Grahek, F. E., Ridley, B. A., Baumgardner, D., Twohy, C. H., Gandrud, B., and Jensen, E. J.: Uptake of NO_y on wave-cloud ice particles, Geophys. Res. Lett., 25, 1725–1728, 1998.

Ziereis, H., Minikin, A., Schlager, H., Gayet, J. F., Auriol, F., Stock, P., Baehr, J., Petzold, A., Schumann, U., Weinheimer, A., Ridley, B., and Ström, J.: Uptake of reactive nitrogen on cirrus cloud particles during INCA, Geophys. Res. Lett., 31, L05115, doi:10.1029/2003GL018794, 2004.

Ziereis, H., Schlager, H., Schulte, P., van Velthoven, P. F. J., and Slemr, F.: Distributions of NO, NO_x, and NO_y in the upper troposphere and lower stratosphere between 28° and 61° N during POLINAT 2, J. Geophys. Res., 105, 3653–3664, 2000.

Zöger, M., Afchine, A., Eicke, N., Gerhards, M. T., Klein, E., McKenna, D. S., Mörschel, U., Schmidt, U., Tan, V., Tuitjer, F., Woyke, T., and Schiller, C.: Fast in situ stratospheric hygrometers: A new family of balloon-borne and airborne Lyman-α photofragment fluorescence hygrometers, J. Geophys. Res., 104, 1807–1816, 1999.